



FATIGUE CRACK GROWTH AND FRACTURE RESISTANCE OF NARROW GAP PIPE WELDS OF TYPE 304LN STAINLESS STEEL

P.K.Singh^{1*}, Punit Arora¹, V.Bhasin¹, K.K.Vaze¹, D.M.Pukazhendi², P.Gandhi², G.Raghava²

¹ Reactor Safety Division, Bhabha Atomic Research Centre, Mumbai-400085, India

(*pk Singh@barc.gov.in)

² Structural Engineering Research Centre, Chennai-600113, India

ABSTRACT

This paper aims at quantifying the fatigue crack growth rate and fracture resistance behavior of the austenitic stainless steel pipe welds by carrying out full scale pipe weld tests. Superiority of the welds produced by hot wire Gas Tungsten Arc Welding (GTAW) over the existing cold wire GTAW and shielded Metal Arc Welding (SMAW) has also been brought out. Prediction of fatigue crack growth for the cracked pipe using Paris law has also been reported. The fatigue crack growth rate (FCGR) and fracture resistance of stainless steel weld and heat affected zone (HAZ) were evaluated to support the LBB application. Tests were carried out room temperature. FCGR test results showed lower crack growth rate in HAZ and the weld fusion zone compare to the base metal for both types of weld. By analyzing the microstructures in the weld fusion zone and HAZ, their effects on crack growth rate were discussed. Analytical predictions for fatigue crack growth life were made using the Paris constants generated from compact tension specimens. These predictions were made for pipe weld, its heat affected zone and pipe (base). Prediction for fatigue crack growth has been compared with experimental results. Effect of prior fatigue loading on fracture resistance of the pipe was also investigated by carrying out full scale pipe weld tests on hot wire and cold wire GTAW. It has been shown that there is no significant effect.

INTRODUCTION

Shielded Metal Arc Welding (SMAW) is one of the widely used joining processes in piping system of the nuclear power plants. This welding process is manual in nature and flux is used to shield the molten weld pool during welding. This weld joints prepared using this process may have reduced fracture toughness and higher fatigue crack growth compared to the parent metal because of the entrapment of slag inclusion and porosity. Although utmost care is taken by following the various standards to produce a defect free weld joints but owing to the manual nature of the process, some defects may be undetected during the inspection at the time of welding due to either limitation of the inspection system or human error. Therefore, improving the fracture toughness and the fatigue crack growth of the weld joints are desirable to enhance the life of the piping components/system. Usually fatigue crack growth rate (FCGR) tests are carried out on the base material and the design curves are given in the ASME code [2010]. Effects of various parameters on FCGR are available in literature based on the standard specimen tests [Ellyn 1997]. Earlier few works has been carried out on the carbon steel pipe and stainless steel pipe welds of SAMW and GTAW [Jung et al 2011, Singh et al 2008]. In view of the above, automated hot Wire Gas Tungsten Arc Welding (GTAW) with narrow gap technique was

adopted for welding of the pipes. Thereafter fatigue crack growth and fracture resistance behavior of the pipe welds were investigated. To demonstrate the leak before- break (LBB) design, mechanical properties of the materials of piping systems are required to be evaluated for various regions of weld joints.

EXPERIMENTAL DETAILS

Pipe material was austenitic stainless steel of SA312 type 304LN. Seamless pipes of nominal outer diameter 324 mm (designated as 300NB) and 168 mm (designated as 150NB) having thickness of 27 mm and 14.3 mm respectively were used for carrying out tests. The pipes were in solution annealed condition and conforming to the SA312 specifications of ASME Section II [ASME, (2010)] and Section III [ASME, (2010)]. The chemical composition of the pipe and pipe weld materials are given in Table 1. Most of the tests were carried out on pipe having girth weld at the center and few tests were also carried out on actual pipe (base). Welding of pipes was carried out as per ASME Section IX [ASME, (2010)] of the Boiler and Pressure Vessel Code. Gas Tungsten Arc welding (GTAW) with cold wire and hot wire was followed for welding of 150NB pipe. GTAW (for root pass and few passes) and Shielded Metal Arc Welding (SMAW) (filling passes) were followed for welding of 300NB pipe. Additionally, hot wire GTAW was also used for welding of 300NB pipe. Both sizes of pipe were welded using conventional V-groove (included angle approximately 75°) and narrow groove. ASME Section II does not specify the filler wire for (GTAW) and welding electrode (SMAW) for welding of SS304LN material. Therefore filler wire ER308L and welding electrode E308L specified for 304L were used for welding of pipes under this study. The details of the welding consumables, process and parameters are given in Table 2. The tensile properties of the pipe and pipe weld for each size of pipes are given in Table 3.

Table 1: Chemical composition of material in weight %

Pipe size	Material	C	Mn	Si	P	S	Cr	Ni	N
ASME	304LN	0.03 max	2.0 max	1.0 max	0.045 max	0.03 max	18-20	8-12	0.1-0.16
300NB	304LN	0.024	1.73	0.55	0.022	0.001	18.8	9.25	0.15
150NB	304LN	0.013	1.57	0.36	0.025	0.001	18.6	8.46	0.11
300NB	Weld	0.03	1.1	0.56	0.021	0.01	19.8	14.1	0.1
150NB	Weld	0.03	1.66	0.39	0.017	0.01	19.98	9.97	0.08

Table 2: Welding consumables, process and parameters

Welding parameters	300NB Pipe Weld	150NB Pipe Weld	300NB and 150NB
Welding process	GTAW & SMAW	GTAW	Hot wire GTAW
Filler wire type	ER 308L for GTAW	ER 308L	ER 308L
Electrode type	E308L for SMAW	-	
Filler wire diameter (mm)	3.2, 1.6	1.6, 3.2 mm	1.2 mm
Electrode diameter (mm)	3.15, 4	-	3.2 mm
Welding Current (A)	100-120 DC	120-140 DC	Peak/base = 110/100

			to 160/140
Welding voltage (V)	15 & 24	18-20	8.4
Welding Speed (mm/min)	40-50	50-60	90-110 mm/min
Inert Gas	Argon in GTAW	Argon	Argon

Table 3: Tensile properties of materials

Pipe size	Material	Yield strength (MPa)	Ultimate Tensile Strength (MPa)	% El
300NB	304LN	324	660	63
150NB	304LN	318	650	67
300NB	SMAW	450	593	38
150NB	Cold wire GTAW	400	586	33
150NB	Hot wire GTAW	320	653	-

Microstructure

The micrographs for the different regions such as base, weld and HAZ for cold wire GTAW welds and hot wire GTAW welds are shown in figures 1 (a-h).



Fig 1a: Base metal



Fig 1b: Heat Affected Zone of cold wire GTAW (Conventional V-Groove)

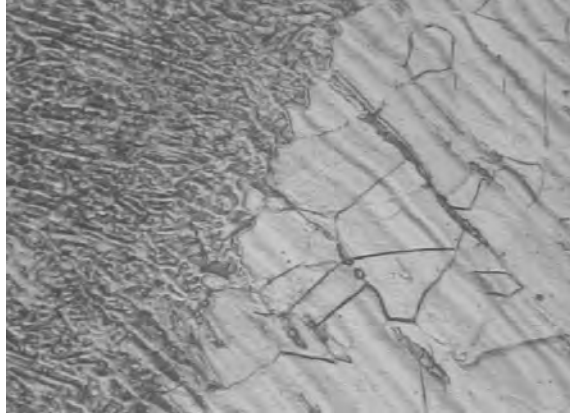


Fig 1c: Weld and Heat Affected Zone of cold wire GTAW (Conventional V-Groove)

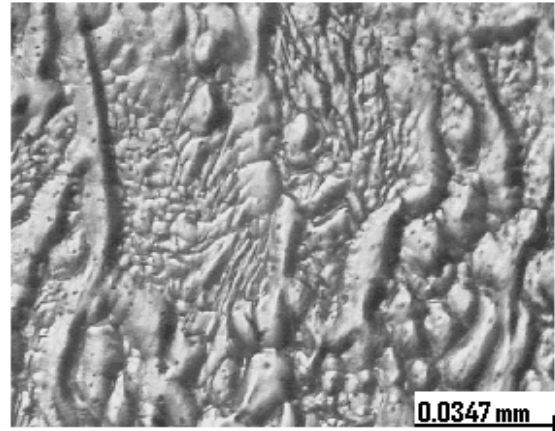


Fig 1d: Weld of cold wire GTAW (Conventional V-Groove)

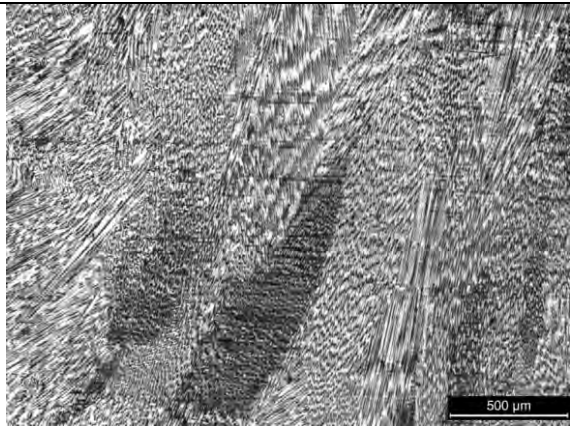


Fig 1e: Weld of Hot wire GTAW (Narrow Gap)

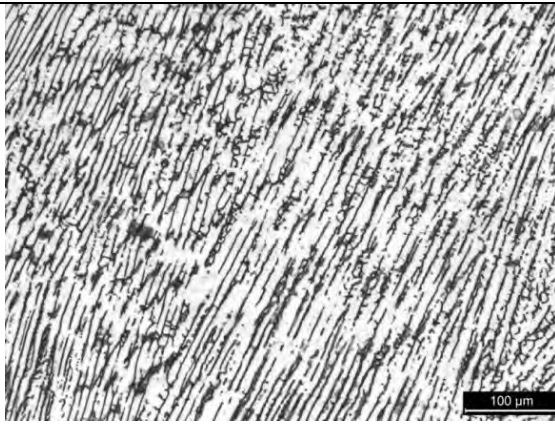


Fig 1f: Dendritic structure in weld of Hot wire GTAW (Narrow Gap)-higher magnification

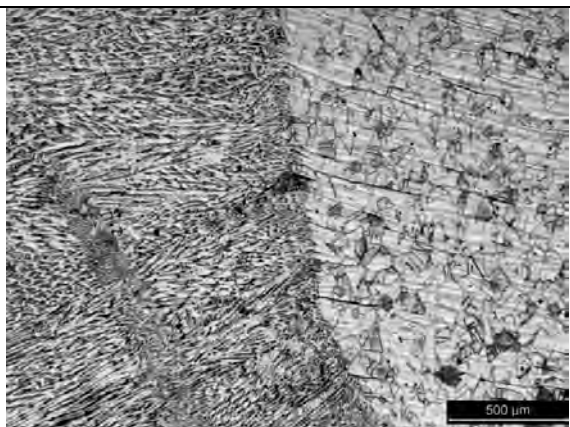


Fig 1g: Weld and Heat Affected Zone of hot wire GTAW (Narrow Gap)

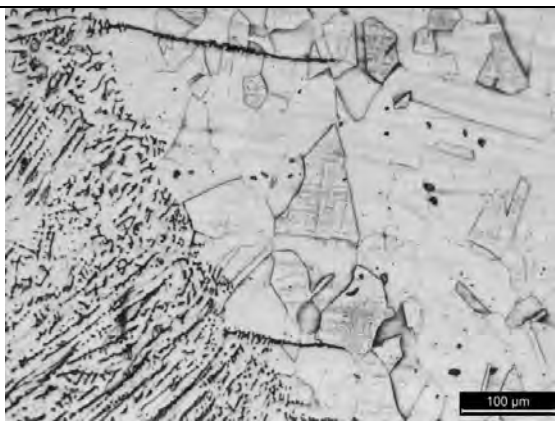


Fig 1h: Weld and Heat Affected Zone of hot wire GTAW (Narrow Gap)-higher magnification

FATIGUE CRACK GROWTH RATE

Details of Pipe Tests

Two sizes of pipe having 170 mm and 324 mm outer diameters were used for tests. Pipe and pipe welds had surface notches of different sizes machined at the outer surface in the circumferential direction by Electro Discharge Machining (EDM). The location of the notch, the shape of the notch (in terms of $2C/a$ and a/t) and other details for all the tests are given in Table 4. Typical specimen and its cross section are shown in figures 2 a and b.

Table 4: Details of the austenitic stainless steel pipe and pipe welds with crack

Test no.	Notch location	OD (mm)	Thickness (mm)	Outer span (mm)	Inner span (mm)	2C (mm)	a (mm)	2C/a	a/t
SPB6-1	Base	170	14.55	1700	680	36	3.5	10	0.24
SPW6-2	Weld (Hot wire GTAW)	170	14.44	1700	680	36	3.5	10	0.24
SPHZ6-3	Weld (Hot wire GTAW)	167	14.54	1700	680	36	3.5	10	0.25
PW6-7	Weld (Cold wire GTAW)	170	14.25	1700	680	44	3.62	12	0.25
PB6-9	Base	168	14.8	2000	680	36	3.6	10	0.24
PW12-10	Weld (SMAW)	324	28.5	5000	1300	123	10.9	11.3	0.38
PB12-12	Base	324	28.12	4000	1300	120	10.9	11.8	0.38

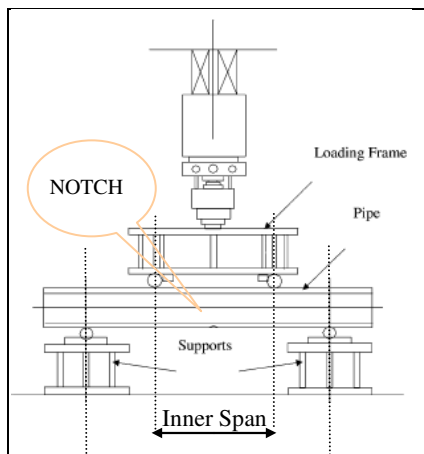


Fig 2a: Schematic of Test Setup

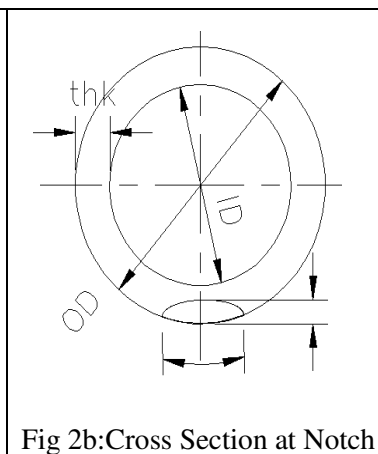


Fig 2b: Cross Section at Notch



Fig 2c: Actual Test Setup

Test Set-Up and Procedures

The test set up is shown in figure 2c. It consists of a servo hydraulic loading system, support for the specimen and various instruments for measurement of data. The support system consists of two pedestals with two rollers and a pair of inner loading rollers, which provides four-point bending. The test specimen was gripped between rollers. This type of loading ensures that the mid section of the specimen, where the notch is located is subjected to pure bending.

The crack depth all along the notch length at several locations (distance between the location was 3-10 mm) was recorded during the fatigue crack growth test with the help of a micro-gauge working on the principle of the Alternating Current Potential Difference (ACPD) technique. The shape of the crack front was obtained by connecting the crack depth readings at several locations for a given number of loading cycles. The load and number of cycles corresponding to each crack depth was also recorded. Load was measured directly using a strain gauge based load cell. Crack growth at the surface (i.e. crack tip) was measured by video-microscope.

Test Conditions

Tests were carried out at room temperature and air environment under load control mode using sinusoidal waveform loading. The constant amplitude method with stress ratios of 0.1 and frequencies in the range of 0.5 to 1.0 Hz was applied. The stress amplitude applied during the test is given in table 5.

Table 5: Details of the test results austenitic pipe and pipe welds with crack

Test no.	Control	Load (KN)		Stress range (MPa)	Stress ratio	No. of Cycles to through wall
		Max	Min			
SPB6-1	Load	258	25.8	234	0.1	39000
SPW6-2	Load	258	25.8	234	0.1	85000
SPHZ6-3	Load	258	25.8	234	0.1	69000
PW6-7	Load	258	25.8	234	0.1	80000
PB6-9	Load	185	18.5	230	0.1	52000
PW12-10	Load	460	50	261	0.1	9500
PB12-12	Load	460	50	263	0.1	55000

Results

The loading details followed during the pipe and pipe weld tests are given in Table 5. Fatigue crack growth tests were continued for the pipe and pipe welds till the crack depth reached through-wall. During the tests crack growth in depth and surface (circumferential) direction with respect to number of cycles was recorded. Maximum crack depth and number of cycles for a given stress ratio (R) of 0.1 are shown in figures 3 to 6. Figure 3 shows the crack growth in base material, heat affected zone and weld produced by hot wire GTAW. Figure 4 shows the crack growth in base and weld metal (cold wire GTAW). Figure 5 shows the crack growth in base and weld metal (SMAW). Figure 6 shows comparison of the V-groove weld and narrow gap weld produced by cold wire GTAW and hot wire GTAW respectively.

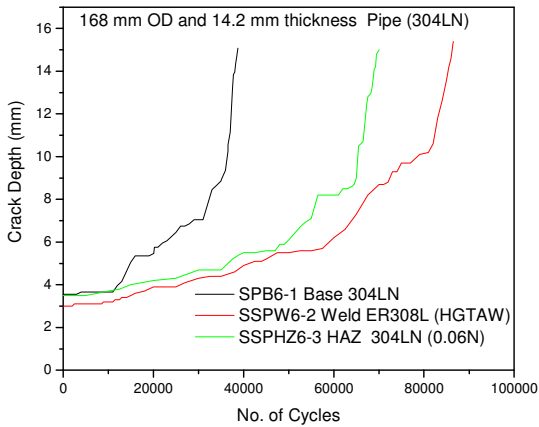


Fig 3: Crack growth in narrow gap welds produced by hot wire GTAW

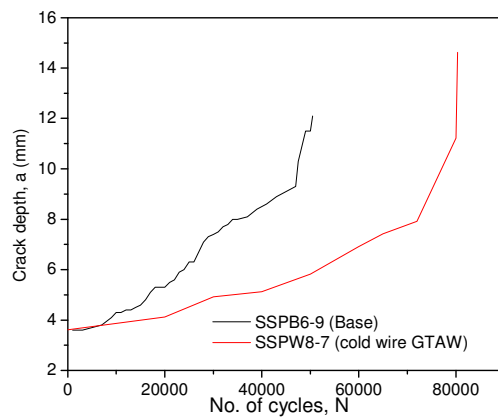


Fig 4: Crack growth in narrow gap welds produced by hot wire GTAW

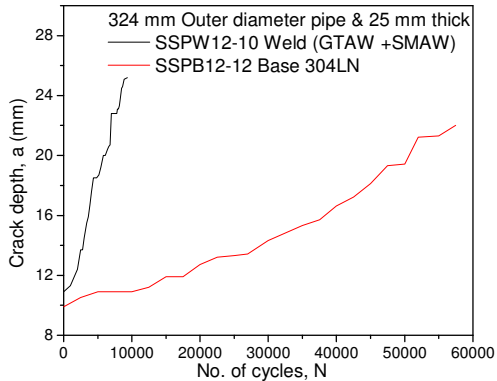


Fig 5: Crack growth in narrow gap welds produced by hot wire GTAW

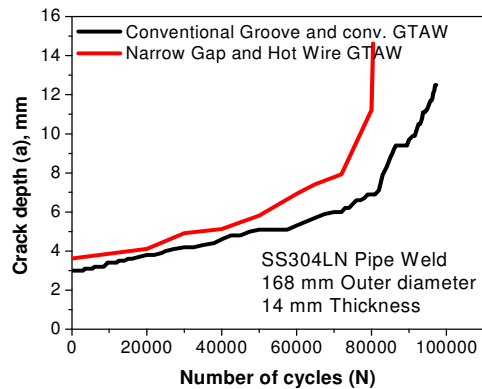


Fig 6: Comparison of crack growth cold wire (V-groove) and hot wire (narrow gap) GTAW

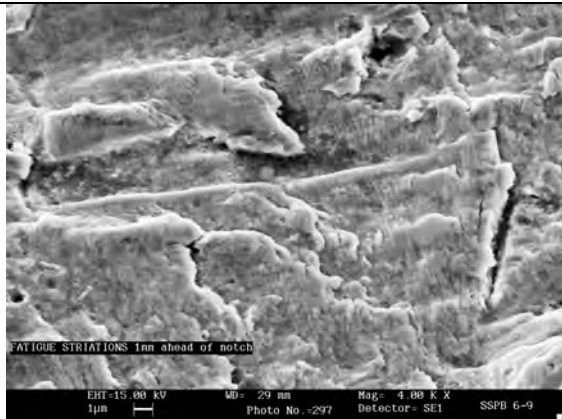


Fig 7a: Fatigue surface near notch (SSPB6-9)

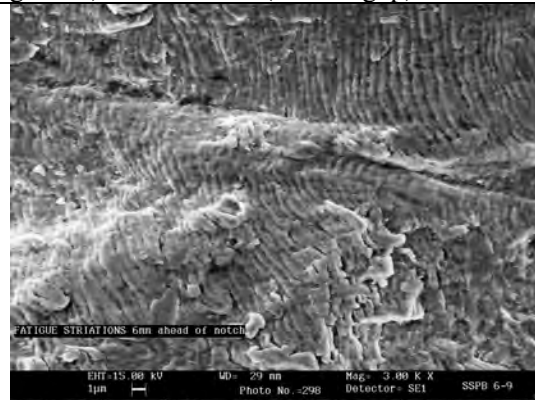


Fig 7b: Fatigue surface away from notch (SSPB6-9)

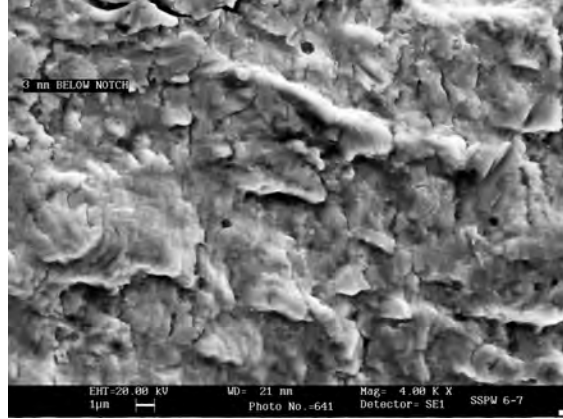


Fig: 7c: Fatigue surface near notch (cold wire GTAW)-SSPW6-7

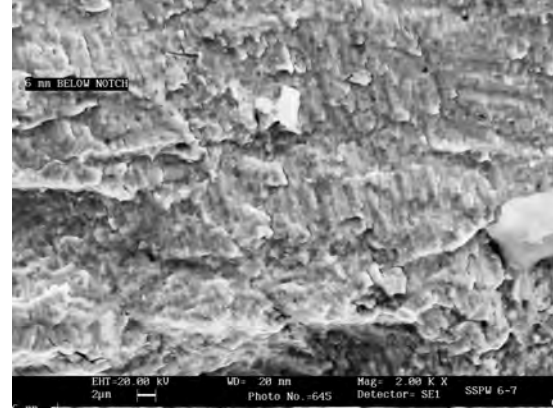


Fig: 7d: Fatigue surface away from notch (cold wire GTAW)-SSPW6-7

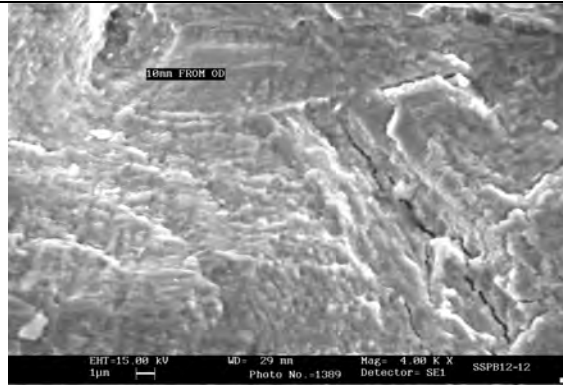


Fig: 7e: Fatigue fracture surface (SSPB12-12)

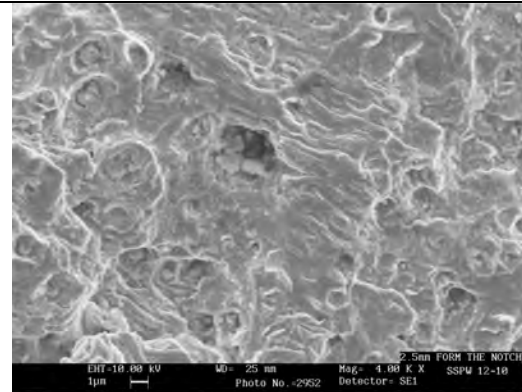


Fig: 7f: Fatigue fracture surface (SMAW)-SSPW12-10

Discussion

Figure 3 shows that crack growth in base metal is higher compared to the weld metal and HAZ in case of the weld produced by hot wire GTAW with narrow gap technique. Figure 4 also shows that the crack growth in case of cold wire GTAW (conventional) is also lower compared to that of weld metal. The source of the base metal (SS304LN) used for the weld joints using hot wire and cold wire GTAW are different. Therefore it has been compared separately. Both the welding process (hot wire and cold wire GTAW) shows the superior crack growth resistance with respect to base metal. Figure 5 shows the crack growth in case of weld produced by SMAW. The crack growth resistance of the weld (SMAW) is very inferior compared to that of the base metal. This is because of the lower ductility of the weld metal compared to that of the base metal. As we know that austenitic stainless steel in solution annealed conditions have equi-axed grain structure as shown in figure 1a. These equi-axed grains get coarsened in the HAZ of the weld as shown in figures 1 (b, c and h). The crack growth in case of weld metal will be same in any direction with respect to pipe axis because of its equi-axed nature. Since the size of the grain become larger in the HAZ, crack growth is lowered because the path of the growing crack is more zig-zag which leads to the reduction in the effective stress intensity factor. The reduction in SIF is due to the inclined nature of the crack tip with respect to the loading direction. In other words, if we have global loading with respect to the crack direction as Mode I, because of the zig-zag nature of the crack growth local stress intensity factor is no more Mode I. It is known that mode I loading is most deleterious for the faster crack growth. The crack growth may be transgranular or intergranular depending upon the weak

link ahead of the crack tip. This leads to the Weld metal have dendritic structure which has directional effect. In this case crack front may not be oriented along the weak link of the dendrite. Here also crack growth is transdendritic or inter-dendritic depending upon the orientation of the dendrite ahead of the crack tip. Weld metal also has few percent of ferrite which helps in retarding the crack growth. It has also been reported that at lower (ΔK), fatigue crack growth is affected by microstructure and continuous striations are not formed on the fracture surface. When the crack driving force is higher than the plastic zone formation effect of microstructure is not significant. This has been observed in present investigation also. The fractographs of the fatigued fracture surfaces ahead of notch tip and away from the notch tip are shown in figures 7 (a-f)

The crack growth observation in base and weld metal is consistent with the observation by various investigators who has shown that crack growth in base metal for austenitic stainless steel [Singh et al (2008)], Nickel alloys [Choudhary et al 2004] and ferritic stainless steel [Ki H et al, 2008] is higher compared to the corresponding weld metal produced by GTAW. Investigators [Changheui J et al (2010)] have also reported that residual stress would also effect the crack growth depending upon its nature (tensile or compressive). Since residual stresses are in equilibrium across section, this will also lead to uneven crack front which in turn will reduce the effective crack driving force (SIF)

PREDICTION OF FATIGUE CRACK GROWTH RATE

The Paris law has been used for the prediction of fatigue crack growth life. To carry out the analysis, Paris constants determined for pipe (base) materials using Compact Tension (CT) specimens machined from the actual pipe/ pipe weld have been used. Analyses have been carried out to predict the fatigue crack growth life of the austenitic stainless steel pipes/ pipes welds (hot wire GTAW and cold wire GTAW) having part through cracks on the outer surface. In the analyses, Stress Intensity Factors (K) has been evaluated through two point approach (i.e at the maximum depth and surface). The scheme considers the ' K ' evaluations at two points of the crack front i.e. maximum crack depth and crack tip at the outer surface. The second scheme-C accounts for the area averaged root mean square stress intensity factor (K_{RMS}) at deepest and surface points. The experimental and analytical results for the crack growth are shown in figures 8 and 9. In these figure ACPD indicates experimental crack growth measured using alternating current potential difference technique. It has been found that the crack growth prediction using this approach is closer to experiment.

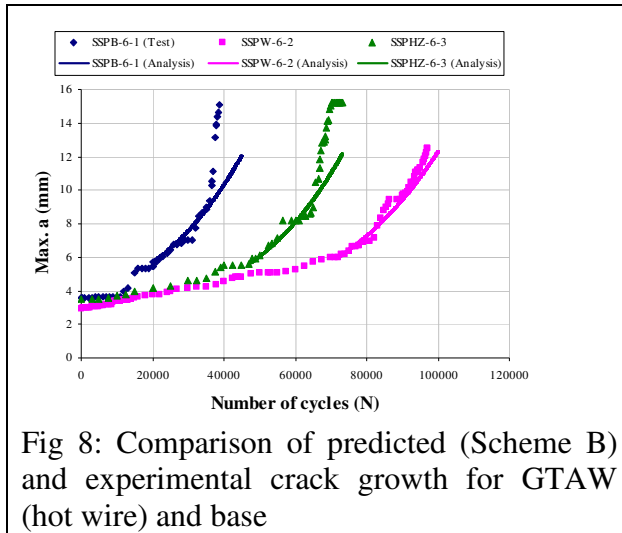


Fig 8: Comparison of predicted (Scheme B) and experimental crack growth for GTAW (hot wire) and base

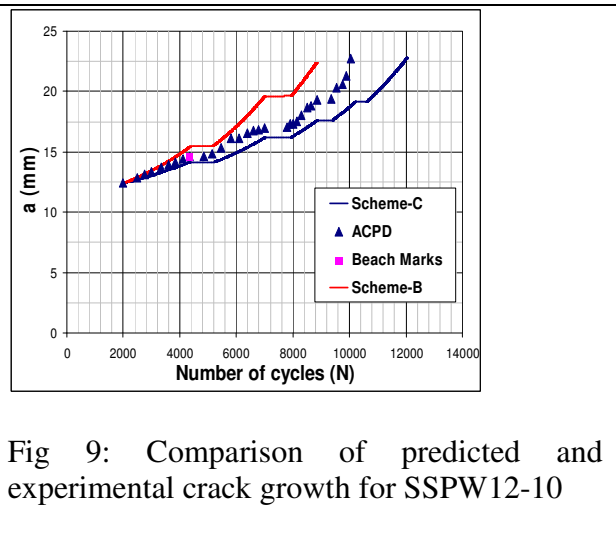


Fig 9: Comparison of predicted and experimental crack growth for SSPW12-10

In figure 8, Paris Constants obtained for the base metal has been used for weld also. But in figure 9, Paris constant evaluated from the weld has been used.

FRACTURE RESISTANCE BEHAVIOUR

Fatigue tests on the surface cracked pipe were carried out till the crack has propagated through thickness till the crack angle was 45° (i.e. one-eighth of the circumference). Thereafter the through thickness cracked pipe and pipe welds of the types listed in table 4 were subjected to monotonic loading to understand the effect of the fatigue loading on the fracture resistance behavior of the pipe and pipe welds. In addition to this few virgin (without prior fatigue loading) pipe and pipe weld were also tested. The load verses load line displacement, rotation were recorded during the tests. Additionally crack growths were also measured using the imaging technique. The load verses load line displacement for the cracked pipe welds for the base and weld (hot wire GTAW) is shown in figure 10. Figure 10 shows almost no difference in the fracture behavior of the weld metal and base metal which is desirable. Load verses load line displacement for fatigued and virgin pipe is shown in fig 11. There is no significant effect of the prior fatigue loading on the fracture resistance behavior of the pipe weld. Fatigued pipe has marginally higher load bearing capacity compared to that of the virgin pipe. Carbon steel pipe shows the reduction in fracture resistance when pipe is subjected to fatigue loading prior to fracture tests [Singh et al 2003].

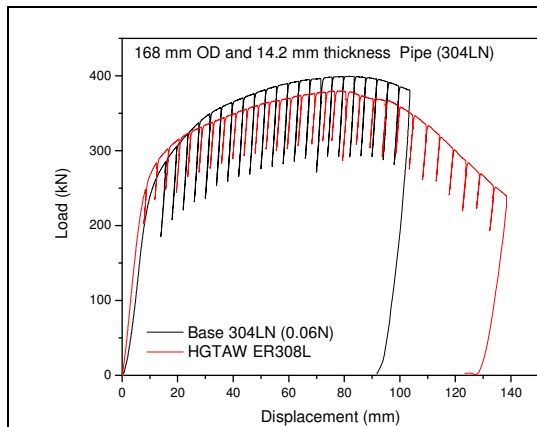


Fig 10: Load verses load line displacement of base and weld (hotwire GTAW)

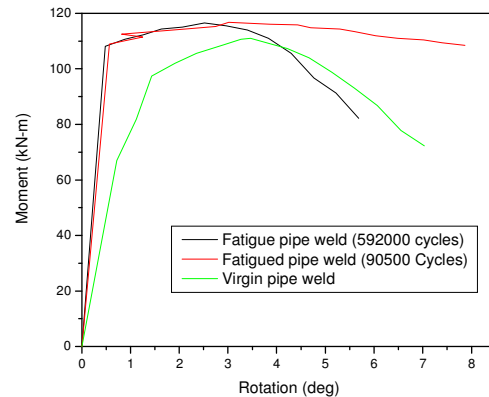


Fig 11: Load verses load line displacement of virgin and fatigue tested pipe weld with crack

The fractographic examination conducted on the tested pipes has shown dimple which is the feature of the ductile failure. Weld and base metal both have shown similar fracture feature as shown in the figure 12 and 13.

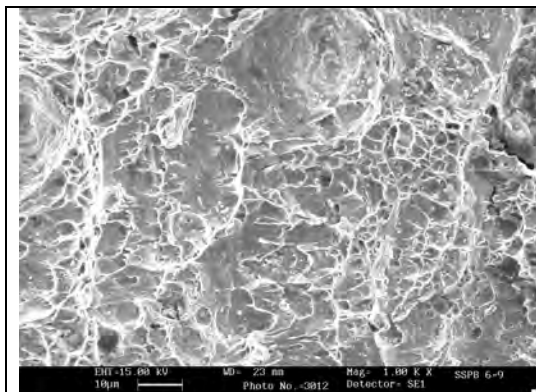


Fig 12: Fracture surface of the base metal (pipe)

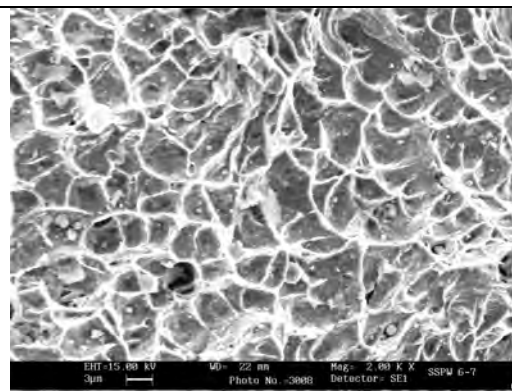


Fig 13: Fracture surface of the weld metal (GTAW)

CONCLUSION

1. FCGR test results showed lower crack growth rate in HAZ and the weld fusion zone compare to the base metal.
2. Predicted fatigue crack growth life compares well with the full scale pipe test results.
3. Prior fatigue loading has no significant effect on the fracture resistance.

REFERENCES

- ASME (2010). "Rules for construction of Nuclear Power Plant Components" ASME Boiler and Pressure Vessel Code, Section II New York, USA.
- ASME (2010). "Rules for construction of Nuclear Power Plant Components" ASME Boiler and Pressure Vessel Code, Section III New York, USA.
- ASME (2010). "Rules for construction of Nuclear Power Plant Components" ASME Boiler and Pressure Vessel Code, Section IX New York, USA.
- Ellyn Fernand, 1997 "Fatigue damage, crack growth and life prediction", Chapman & Hall, pp 381.
- Ho-Jung Lee, Minu Kim, Changheui Jang, Sun-Young Cho, Jun-Seog Yang, (2011) "Fatigue Crack Growth Rate and Fracture Resistance of Heat Affected Zone of Type 316L Stainless Steel with Narrow Gap Welds" Proceedings of the ASME 2011 Pressure Vessels & Piping Division Conference, Maryland, USA
- P.K.Singh, V.Bhasin, K.K.Vaze, A.K.Ghosh (2008) "Fatigue Studies on Austenitic Stainless Steel Pipe Welds" International Congress 2008, International Institute of welding, Chennai
- Singh P.K., Vaze K.K., Bhasin V., Kushwaha H.S, Gandhi. P., Murthy D.S.R (2003) "Crack initiation and growth behaviour of circumferentially cracked pipes under cyclic and monotonic loading" International Journal of Pressure Vessel and Piping 80, Issue 9, 629-640
- Changheui J, Pnung-Yeon Cho, Minukum Seung-Jin Oh, Jun Seog Yang (2010) "Effect of microstructure and residual stress on FCG of stainless steel narrow gap welds" Material & Design 31, 1862-1870.
- Choudhary B., Roedig M., Mannan S.L. (2004) "Fatigue crack growth behavior of base metal, weld metal and heat affected zone of Alloy 800 at 823K", Trans Indian Inst. Met., Vol 57. No.6, 639-649.
- Ki H. Kim C.S, Jeon Y.C SIKWUM (2008), "Fatigue crack growth characteristics in dissimilar weld metal" Material Science Forum, Vol 580-582, 593-596